blood

2008 111: 4542-4550
Prepublished online Feb 21, 2008;
doi:10.1182/blood-2007-06-094763

Angiogenic endothelium shows lactadherin-dependent phagocytosis of aged erythrocytes and apoptotic cells

Marcel H. A. M. Fens, Enrico Mastrobattista, Anko M. de Graaff, Frits M. Flesch, Anton Ultee, Jan T. Rasmussen, Grietje Molema, Gert Storm and Raymond M. Schiffelers

Blood (print ISSN 0006-4971, online ISSN 1528-0020), is published semimonthly by the American Society of Hematology, 1900 M St, NW, Suite 200, Washington DC 20036.

Angiogenic endothelium shows lactadherin-dependent phagocytosis of aged erythrocytes and apoptotic cells

Marcel H. A. M. Fens,[1] Enrico Mastrobattista,[1] Anko M. de Graaff,[2] Frits M. Flesch,[1] Anton Ultee,[3] Jan T. Rasmussen,[4] Grietje Molema,[5] Gert Storm,[1] and Raymond M. Schiffelers[1]

[1]Department of Pharmaceutics, Utrecht Institute for Pharmaceutical Sciences (UIPS), Utrecht University, Utrecht, The Netherlands; [2]Department of Biochemistry and Cell Biology, and [3]Department of Pathobiology, Faculty of Veterinary Medicine, Utrecht University, Utrecht, The Netherlands; [4]Protein Chemistry Laboratory, Department of Molecular Biology, Aarhus University, Aarhus, Denmark; and [5]Department of Pathology and Laboratory Medicine, Medical Biology Section, University Medical Center Groningen, University of Groningen, Groningen, The Netherlands

Angiogenic endothelium plays a crucial role in tumor growth. During angiogenesis, complex alterations in the microenvironment occur. In response, the endothelium undergoes phenotypic changes, for example overexpression of α_v-integrins. Here, we show that the overexpression of α_v-integrins on angiogenic endothelial cells is engaged in phagocytic actions involving binding ("tethering") and uptake ("tickling") of lactadherin (also termed MFG-E8)–opsonized particles. Phosphatidylserine (PS)–exposing multilamellar vesicles, "aged" erythrocytes, and apoptotic melanoma cells incubated with lactadherin were all phagocytosed by angiogenic endothelial cells in vitro. Furthermore, we demonstrated lactadherin expression in and around tumor blood vessels making opsonization in situ plausible. By engineering the surface of erythrocytes with covalently coupled cyclic Arg-Gly-Asp (RGD) peptides—mimicking lactadherin opsonization—we could induce phagocytosis by angiogenic endothelial cells both in vitro and in vivo. In vitro, this was confirmed by cytochalasin D preincubation. When RGD-erythrocytes were administered intravenously in tumor-bearing mice, blood vessel congestion followed by tumor core necrosis was seen. Moreover, RGD-erythrocytes could delay tumor growth in a murine melanoma model, possibly through induction of tumor infarctions. These results reveal that angiogenic endothelial cells have phagocytic properties for lactadherin-opsonized large particles and apoptotic cells. Implications of our findings for diagnostic and therapy of angiogenesis-driven diseases are discussed. (Blood. 2008;111:4542-4550)

Introduction

Cells that are going into apoptosis expose phosphatidylserine (PS) on their surface that serves as an "eat me" signal for both professional phagocytes (such as macrophages, B lymphocytes, and immature dendritic cells) and nonprofessional phagocytes (such as fibroblasts and epithelial cells).[1] Phagocytes recognize apoptotic cells directly via the PS receptor or indirectly via α_v-integrins that are present on the phagocyte surface.[2] In the latter process, $\alpha_v\beta_3$ and $\alpha_v\beta_5$ integrins recognize PS through an opsonin called lactadherin, also known as milk fat globule epidermal growth factor-8 (MFG-E8).[3,4] This opsonin contains a PS-binding C-domain and an RGD-motif present in the epidermal growth factor domain, which binds to $\alpha_v\beta_3$ and $\alpha_v\beta_5$ integrins.[2,5-7] Rapid clearance of apoptotic cells prevents the release of potentially harmful or immunogenic intracellular materials from these cells.[8] Lactadherin-deficient mice have shown impaired phagocytosis of apoptotic cells, induction of autoimmune diseases, and autoantibody production.[9,10] α_v-Integrins are densely present on macrophages and dendritic cells and play an important role in phagocytosis.[11] Notably, these integrins are also overexpressed on angiogenic endothelium[12] where they play an important role in cell adhesion and migration.[13,14] Recently, Silvestre et al discovered that lactadherin is expressed in and around (angiogenic) blood vessels in an ischemic hind limb model and that the protein seems to play a crucial role in vascular endothelial growth factor (VEGF)–dependent neovascularization.[15] As angiogenesis is also a hallmark of tumor growth and tumor angiogenic endothelium expresses α_v-integrins, in this study we have explored the possible role of lactadherin-induced phagocytosis by angiogenic tumor endothelial cells.

Methods

Cell lines

B16.F10 murine melanoma cells (ATCC, Manassas, VA) were cultured on regular FCS-enriched DMEM. Human umbilical vein endothelial cells (HUVECs) were cultured on EGM-2 endothelial cell growth medium-2 (Cambrex, East Rutherford, NJ) consisting of EBM-2 medium supplemented with an EGM-2 bullet kit (containing growth factors, 2% FBS, and antibiotics). HUVECs were used as an $\alpha_v\beta_3$-expressing model for proliferating endothelium to a maximal passage number of 8.

Lactadherin purification

Bovine lactadherin was purified as previously described.[16] Purity was checked by sodium dodecyl sulfate–polyacrylamide gel electrophoresis (SDS-PAGE) and N-terminal amino acid sequencing and shown to be

Submitted June 8, 2007; accepted February 13, 2008. Prepublished online as *Blood* First Edition paper, February 21, 2008; DOI 10.1182/blood-2007-06-094763.

The online version of this article contains a data supplement.

The publication costs of this article were defrayed in part by page charge payment. Therefore, and solely to indicate this fact, this article is hereby marked "advertisement" in accordance with 18 USC section 1734.

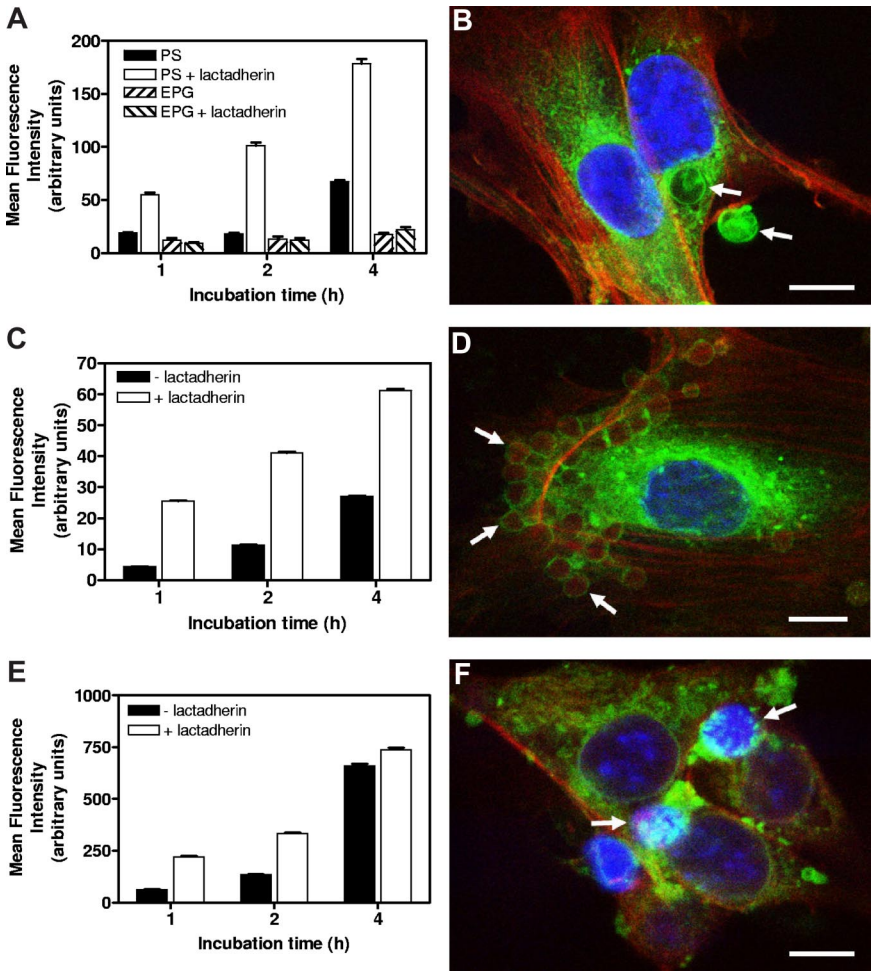

Figure 1. Lactadherin-mediated association of PS-exposing particles and cells in vitro by endothelial cells. (A) DiD-labeled MLVs containing either PS or EPG, preincubated in the presence or absence of lactadherin, were incubated with endothelial cells. Only in the case of PS-MLVs was enhanced association of lactadherin-preincubated MLVs (values ± SEM) seen. Association increased in time. (B) Multiphoton image of an endothelial cell with bound and internalized lactadherin-opsonized approximately 2 μm sized PS-MLVs (indicated by arrows) after 2 hours of incubation. Scale bar represents 5 μm. (C) Endothelial cell association of PKH-26–labeled aged erythrocytes with or without preincubation with lactadherin. Lactadherin enhanced endothelial cell association in a time-dependent manner (values ± SEM). (D) Multiphoton image of an endothelial cell with associated opsonized aged erythrocytes (indicated by arrows) after 4 hours of incubation. Scale bar represents 10 μm. (E) Endothelial cell association of PKH-26–labeled apoptotic tumor cells with or without preincubation with lactadherin (values ± SEM). Lactadherin enhanced endothelial cell association in a time-dependent manner. (F) Multiphoton image of endothelial cells with associated apoptotic tumor cells (indicated by arrows) that show a typical condensed nuclear staining after 4 hours of incubation. Scale bar represents 10 μm.

97% to 98%, in 2 glycosylation forms. Protein concentrations were determined by amino acid analysis based on o-phthaldialdehyde derivatization.

Particle and cell preparations

Multilamellar vesicles (MLVs) of approximately 2 μm were prepared by hydration with PBS of a lipid film containing DPPC/cholesterol/PS or EPG and Rhodamine phosphatidyl ethanolamine (Sigma-Aldrich, St Louis, MO) or DiD (fluorescence-activated cell sorting [FACS]) in a molar ratio of (2:1:0.3:0.003 mol/mol) using glass beads. Particle size was analyzed by Coulter counter measurements (Beckman Coulter, Hialeah, FL). "Aged" erythrocytes were prepared by overnight glucose starvation (N_2 flushed) of C57Bl/6-derived erythrocytes; finally PKH-26 (Sigma-Aldrich) was used for labeling. Overnight starvation at room temperature (RT) was also applied to obtain apoptotic B16.F10 melanoma cells.

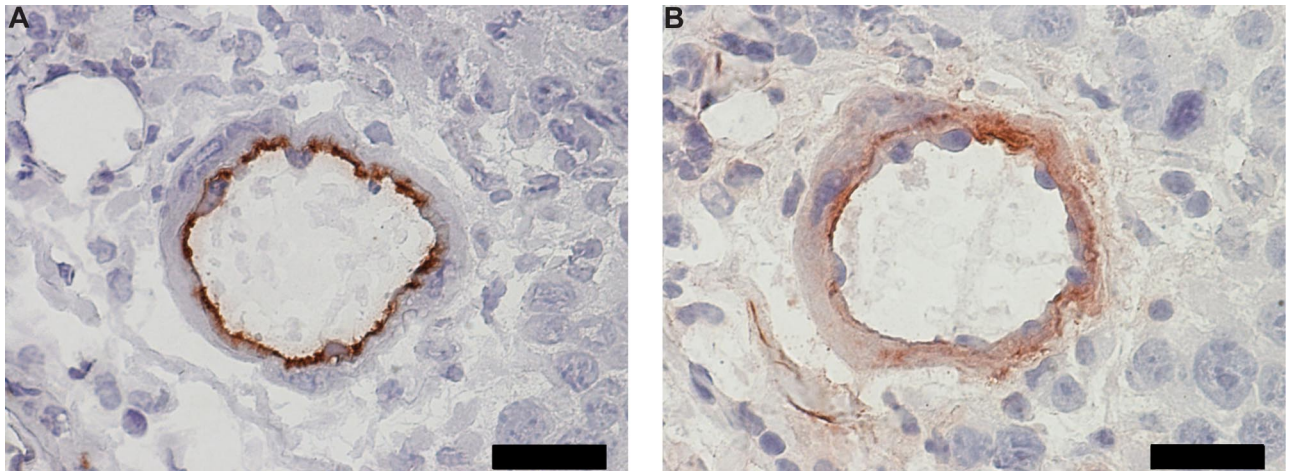

Figure 2. Coexpression of CD31 and lactadherin in tumor vasculature. (A) Immunohistochemical staining for panendothelial cell marker CD31 in a B16.F10 melanoma tissue section. Scale bar represents 20 μm. (B) Immunohistochemical staining for lactadherin in a sequential B16.F10 melanoma tissue section. Scale bar represents 20 μm.

Quantification of phagocytosis by endothelial cells

Fluorescently labeled particles and cells exposing PS were preincubated with 50 μg lactadherin for 30 minutes at RT, followed by centrifugation, removal of unbound PS-containing supernatant, and subsequent incubation with HUVECs. After incubation, cells were washed and trypsinized. Fluorescence measurements were performed using a fluorescence-assisted cell sorting (FACSCalibur; Becton Dickinson, Lincoln Park, NJ); a total of 5000 cells were counted per sample.

Visualization of fluorescently labeled particles and cells associated with endothelial cells

Multilamellar vesicles (MLVs) with Rhodamine phosphatidyl ethanolamine, aged murine (C57Bl/6-derived) erythrocytes, and apoptotic B16.F10 cells labeled with PHK-26 were preincubated with bovine lactadherin (10 μg). After 30-minute incubation at RT, samples were spun down and unbound lactadherin present in the supernatant was removed. Samples were added to HUVECs in chamber slides (LAB-TEK; Nunc, Rochester, NY). Finally, cells were fixed with formaldehyde (4%) containing 1% methanol and nuclei were stained with DAPI (blue) and actin was stained (red) with Phalloidin 633 (Molecular Probes, Eugene, OR). Slides were mounted with Fluorsave Reagent (Calbiochem, San Diego, CA). Fluorescent signals were visualized using a multiphoton system (Bio-Rad, Hemel Hempstead, United Kingdom). Excitation of the DAPI was achieved by multiphoton excitation at 780 nm using a mode-locked Titanium:Sapphire laser (Tsunami; Spectra Physics, San Jose, CA) pumped by a 10-W solid state laser (Millennia Xs; Spectra Physics), whereas the Rhodamine PE, PKH-26, and Phalloidin 633 were excited by confocal lasers. Samples were viewed with a TE200 inverted microscope using a 60×/1.4 oil objective (Nikon, Tokyo, Japan). Images were analyzed using LaserSharp 2000 software (Bio-Rad).

Coupling of RGD- or RAD-peptides to the erythrocyte surface

We collected whole mouse blood by cardiac puncture of C57Bl/6 mice and isolated the red blood cells by centrifugation (1000*g*, 10 minutes, 4°C). Coupling of the peptides was according to Coller et al.[17] In brief, after washing in isotonic buffer (140 mM NaCl, 5 mM KCL, 10 mM glucose, and 10 mM $NaPO_4$, pH 7.4), erythrocytes were incubated with 0.5 mg sulfoEMCS, a hetero-bifunctional cross-linking reagent (Uptima, Montluçon Cedex, France), per milliliter of erythrocytes (hematocrit value ± 95%) for 100 minutes at RT on a roller bench. Finally, erythrocytes were incubated with cyclic RGD- or cyclic RAD-peptide (JPT Peptide Technologies, Springfield, VA) for 30 minutes at room temperature, after deacetylation of the peptides in 0.5 M hydroxylamine in 0.5 M HEPES buffer (pH 7.0), and unbound peptide was removed by repeated washing.

Immunohistochemical lactadherin, CD31, and RGD staining

After acetone fixation, freeze sections were incubated with monoclonal anti–MFG-E8 (mAb 2422, 1:1000; MBL, Nagoya, Japan [5]) followed by biotinylated goat anti–Armenian hamster antibody (1:200; Santa Cruz Biotechnology, Santa Cruz, CA) and visualized with HRP-labeled streptavidin (1:400, Vector). For CD31 (PECAM-1) panendothelial cell staining, a primary rat anti–mouse CD31 (1:100; Serotec, Raleigh, NC) monoclonal antibody was used followed by a second rabbit anti–rat HRP (1:40; Dako, Carpinteria, CA) and a third goat anti–rabbit HRP antibody (1:100; Dako). For RGD staining, polyclonal anti-RGD antiserum raised in rabbits (1:1000 in PBS/FCS 5% buffer) was used, followed by immunoperoxidase staining by a second goat anti–rabbit horseradish peroxidase (HRP, 1:100; Dako) and a third rabbit anti–goat HRP antibody (1:100; Dako). In all staining procedures, 3-amino-9-ethylcarbazole (AEC) was used as a substrate. Sections were viewed with an Eclipse TE2000-U inverted microscope using a 60×/1.4 oil objective (Nikon). Images were analyzed using NIS elements BR 2.3 software (Nikon).

SDS-PAGE and Western blotting

We treated control and RGD-coupled erythrocyte lysates with reducing SDS sample buffer before running on SDS-PAGE 12% gel (100 Volt, 2 hours, Criterion XT Precast gel; Bio-Rad). Identical samples on gels were used for either Coomassie blue staining or Western blotting (iBlot; Invitrogen, Frederick, MD). Polyclonal rabbit anti-RGD antiserum (1:1000) followed by goat anti–rabbit HRP (1:250; Dako) were used for immunostaining of the blotted membranes.[18,19]

Scanning electron microscopy

HUVECs were fixed with Karnovsky fixative directly after sample incubation and washing. Next, cells were washed with 0.1 M cacodylate buffer followed by OsO4 2%, tanine 1%, and OsO4 1% incubation. After dehydration by acetone, critical drying of the samples was performed and finally an approximately 10-nm film of platinum was sprayed on the samples. We digitally photographed all images at 5.0 kV on a XL30FEG (FEI, Hillsboro, OR) using an ultra-high-resolution mode. Images were analyzed using analySIS software.

Light microscopy

HUVECs were seeded in 16-well chamber slides 24 hours before start of the experiments. After sample incubation, cells were gently washed and fixed in formalin 2%/glutaraldehyde 0.1% (vol/vol). Finally, cells were H&E stained, and paraffin-embedded tissue samples were cut in 5-μm thin sections and stained with H&E. Samples were viewed with a BX50 microscope (Olympus, Tokyo, Japan; 10×/0.30, 40×/0.75, and 100×/1.3 oil objectives).

Transmission electron microscopy (TEM)

Samples were collected and fixed in 2% glutaraldehyde. Next, samples were postfixed with 2% glutaraldehyde in 0.1 M sodium cacodylate buffer after OsO4 4% and uranyl 2% treatment. Finally, after dehydration, samples were embedded in durcupan (Fluka, Munich, Germany). We prepared ultrathin (~60 nm) sections, with a Reichert ultracut S ultramicrotome (Leica) and viewed them with a Philips CM10 transmission electron microscope (Philips, Eindhoven, The Netherlands). Images were developed from negatives and digitalized by a Heidelberg Linosan 1450 scanner (Heidelberg, Germany).

In vivo binding of fluorescently labeled erythrocytes

B16F0 tumor–bearing mice (C57Bl/6) were injected intravenously with either plain or RGD-modified DiD-labeled erythrocytes. Four hours after injection mice were killed and tumors were excised and snap frozen in liquid nitrogen. Finally 20-μm freeze sections were cut and examined using a Leica TCS-SP confocal laser scanning microscope equipped with a 633-nm HeNe-laser. Samples were viewed with a Leica TCS-SP microscope using a 40×/1.25 objective. Leica Confocal Software (LCS) was used to acquire images and LCS-lite for image analysis.

Inhibition assay

Wortmannin (50 nM; Fluka) and cytochalasin D (10 μM; Sigma-Aldrich) were added in presence of EGM-2 medium to preseeded HUVECs. After 30-minute incubation, the wortmannin and cytochalasin D were removed and the RGD- and lactadherin-erythrocytes were added. Finally, nonassociated erythrocytes were removed 1 hour after addition, and HUVECs were trypsinized and analyzed by FACS.

Therapy of subcutaneously grown melanoma tumors

Male C57Bl/6 mice weighing approximately 20 g (Charles River Laboratories, Wilmington, MA) were inoculated with 10^6 B16.F10 cells subcutaneously at day 0. From day 9, when tumor volume averaged 25 mm^3, mice were intravenously treated (every second day) with 200 μL approximately 90% hematocrit erythrocyte suspensions. Tumor sizes were measured every second day, and volumes were calculated using the following equation: $V = (a \times 0.52) \times b^2$, where a is the largest superficial diameter and b the

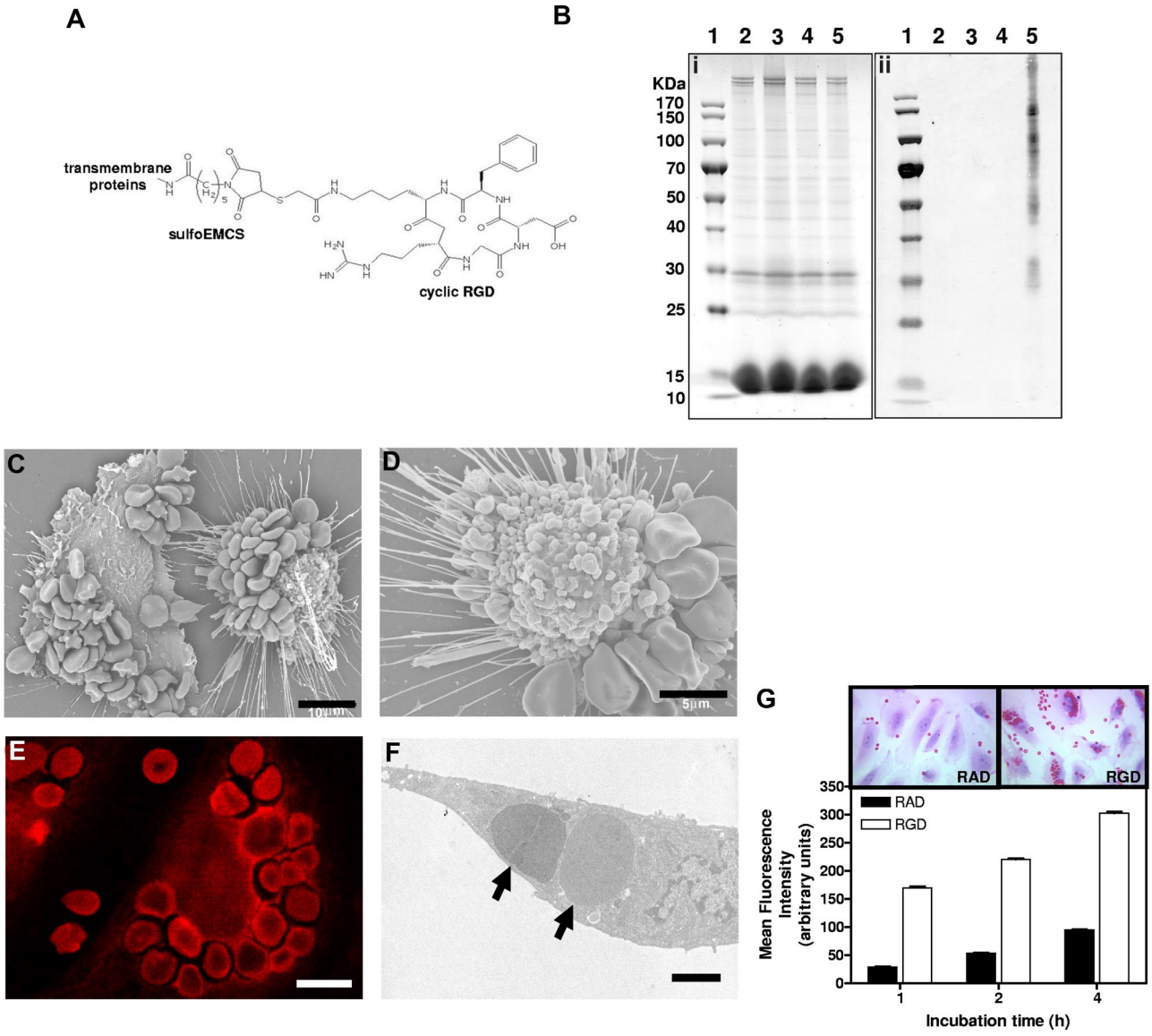

Figure 3. In vitro binding and erythrophagocytosis of RGD-modified erythrocytes by endothelial cells. (A) Structural formula of cyclic RGD-peptide coupled to erythrocyte transmembrane proteins via a sulfoEMCS heterobifunctional cross-linker. (B) SDS-PAGE gel (i) and anti-RGD antiserum-stained immunoblot (ii) of control untreated erythrocytes (lane 2), erythrocytes with sulfoEMCS linker (lane 3), erythrocytes with RGD (lane 4), and erythrocytes with sulfoEMCS linker and RGD (lane 5) lysates. The sizes of the bands of the PageRuler protein ladder (lane 1) are shown next to the SDS-PAGE gel. The corresponding immunoblot shows association of RGD-peptides with multiple transmembrane proteins only for the erythrocytes that contained both the sulfoEMCS linker and the RGD-peptides. (C) Scanning electron microscopy image of extensively bound RGD-erythrocytes to the endothelial cell membrane after 1-hour incubation. Scale bar represents 10 μm. (D) Retracted endothelial cell with bound RGD-erythrocytes, showing extensive blebbing as a sign of cytotoxicity that can already be observed after 30 minutes. Scale bar represents 5 μm. (E) Confocal microscopy image of autofluorescence of RGD-erythrocytes taken up by an endothelial cell after 4-hour incubation, demonstrating that cell binding is followed by erythrophagocytosis. Scale bar represents 10 μm. (F) Transmission electron microscopy (TEM) image of phagocytosed RGD-erythrocytes (➡) in an endothelial cell after 1-hour incubation. Scale bar represents 2 μm. (G) Endothelial cell association of RAD- and RGD-modified erythrocytes. RGD-erythrocytes displayed enhanced binding at all time points compared with control RAD-erythrocytes (values ± SEM). Inserts show representative light microscopy images of erythrocyte-association at 4-hour incubation.

smallest. Mice were killed when tumor volume exceeded 2000 mm^3 or when animals appeared moribund. For histologic evaluation of treatments, mice were killed 4 and 24 hours after first administration; tumors were excised and directly fixed in formaldehyde 4%.

Statistical analysis

Individual tumor growth data were calculated by subtracting initial tumor volume from tumor volumes at the end of the experiment. The data were statistically analyzed by a nonparametric 2-tailed Mann-Whitney test using GraphPad Prism 4 for Windows software (GraphPad Software, San Diego, CA).

Results

Overexpression of α_v-integrins on angiogenic endothelium and presence of lactadherin locally in and around vasculature would make angiogenic endothelial cells capable of α_v-integrin–mediated phagocytosis. We tested this hypothesis by challenging human umbilical vein endothelial cells (HUVECs) with lactadherin-opsonized PS-exposing particles and cells. Multilamellar vesicles (MLVs) containing PS (mean size of 2 μm) showed a markedly increased and time-dependent uptake by

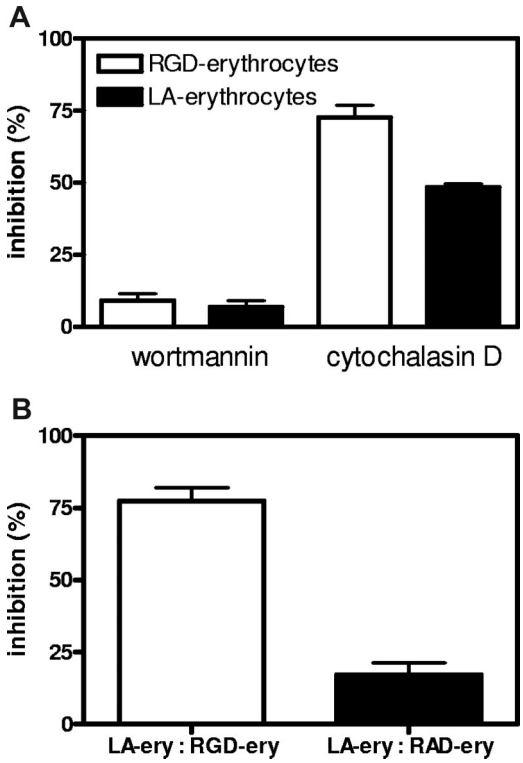

Figure 4. Inhibition and competition of RGD-erythrocytes and lactadherin-erythrocytes for binding and uptake by HUVECs. (A) HUVECs were preincubated with wortmannin (50 nM) and cytochalasin D (10 μM) for 30 minutes followed by 1-hour incubation with PKH-26–labeled RGD-erythrocytes and lactadherin (LA)–erythrocytes. Both RGD-erythrocytes and LA-erythrocytes show the same inhibitor profile, indicating that both are processed by the same internalization route (values mean ± SEM). (B) Lactadherin-erythrocytes were PKH-26 labeled and added to HUVECs in presence of an equal volume (1:1 vol/vol) of unlabeled RAD- or RGD-erythrocytes. After 1-hour incubation at 37°C, samples were removed and wells were washed. Next, cells were detached with trypsin/EDTA and measured by FACS. Percentage of maximum inhibition was calculated and expressed as mean plus or minus SEM.

endothelial cells after preincubation with lactadherin (Figure 1A,B). MLVs exposing egg phosphatidyl glycerol (EPG), a phospholipid that also bears a negative charge but lacking a recognition signal for lactadherin, did not associate with endothelial cells in presence of the opsonin (Figure 1A). In a similar fashion, murine erythrocytes exposing PS, "artificially aged" by glucose and oxygen deprivation, also showed a massive enhanced uptake by endothelial cells after lactadherin opsonization (Figure 1D) compared with nonopsonized erythrocytes, in a time-dependent fashion (Figure 1C). In addition to PS-exposing erythrocytes, we studied apoptotic B16.F10 melanoma cells. Many tumors contain various numbers of endogenous apoptotic tumor cells due to hypoxia and uncontrolled proliferation. These PS-exposing apoptotic tumor cells are likely candidates to be phagocytosed. Pretreatment of apoptotic melanoma cells with lactadherin resulted in binding and uptake by endothelial cells, which increased in time (Figure 1E,F). Taken together, these in vitro experiments demonstrate the phagocytic capacity of endothelial cells toward lactadherin-opsonized PS-exposing particles and cells.

To study our hypothesis in vivo, we investigated the presence of lactadherin in and around tumor tissue; immunohistochemical costaining in serial sections of B16.F10 melanoma tissue showed positive staining for CD31 (panendothelial cell marker) and lactadherin (Figure 2A and B, respectively). Neutzner et al recently showed colocalization of lactadherin and CD31 in Rip1-Tag2 murine pancreatic tumor model.[20] These results make endogenous opsonization plausible. Subsequently, we mimicked lactadherin-opsonized apoptotic cells by engineering the surface of erythrocytes with covalently coupled cyclic RGD (Figure 3A). We have chosen RGD-modified erythrocytes as a model for apoptotic opsonized cells as erythrocytes are small and sufficiently flexible to pass capillaries and can therefore reach angiogenic endothelium after intravenous administration. Moreover, erythrocytes have extensively been used for drug delivery and imaging purposes that facilitate therapeutic applications.[21,22] In addition, RGD-modified erythrocytes may be of interest to for hematologic studies since aged erythrocytes expose PS on the cell surface inducing rapid clearance and PS exposure is involved in hemolytic anemia.[23]

Successful RGD-peptide coupling via sulfoEMCS was confirmed using Western blot, showing that the peptide is attached to the surface of the majority of erythrocyte transmembrane proteins (Figure 3B). The covalent coupling ensures that the recognition signal is stably anchored on the cell surface. Incubation of endothelial cells with RGD-erythrocytes in vitro showed massive binding of 10 to 30 erythrocytes per endothelial cell (Figure 3C). In most cases, the extensive binding was accompanied by retraction and rounding up of the endothelial cells, indicating cytotoxicity (Figure 3C,D). This process already started after 30 minutes of incubation and affected the majority of the endothelial cells present. At later time points, binding of erythrocytes to endothelial cells was followed by erythrophagocytosis, resulting in large numbers of internalized erythrocytes (Figure 3E,F). Notably, during phagocytosis, membrane ruffles were formed in the region of surface bound erythrocytes, which was followed by engulfment (Figure S1A,B, available on the *Blood* website; see the Supplemental Materials link at the top of the online article). Quantification of phagocytic activity of endothelial cells showed a large preference for uptake of RGD-erythrocytes compared with erythrocytes modified with control peptide RAD (Figure 3G). HUVECs that experienced cytotoxicity were lost during washing steps. Erythrocyte uptake by adherent HUVECs increased over time. To look into the internalization route of RGD-erythrocytes and lactadherin-erythrocytes, uptake was studied in the presence of wortmannin and cytochalasin D (Figure 4A). Both RGD-erythrocytes and lactadherin-erythrocytes show the same inhibitor profile, indicating that both are processed by the same internalization route. Based on the size of the internalized cells, 3 processes can in principle be responsible for uptake: macropinocytosis, phagocytosis, and emperipolesis. Wortmannin, a phosphoinositide 3-kinase inhibitor, has been described to primarily affect macropinocytosis and late stages of phagocytosis.[24,25] Cytochalasin D, an actin polymerization inhibitor, affects early stages of (apoptotic cell) phagocytosis, while it does not inhibit emperipolesis.[26] The observation that cytochalasin D strongly inhibits erythrocyte uptake would therefore indicate that phagocytosis is the primary internalization route. By coincubating HUVECs with PKH-26–labeled lactadherin-erythrocytes and unlabeled RGD/RAD-erythrocytes, we evaluated binding site competition (Figure 4B). Only RGD-erythrocytes strongly reduced binding of lactadherin-erythrocytes.

To investigate the binding and uptake by angiogenic endothelium in vivo, RGD-erythrocytes were injected intravenously into B16.F10 melanoma–bearing mice. Microscopic evaluation

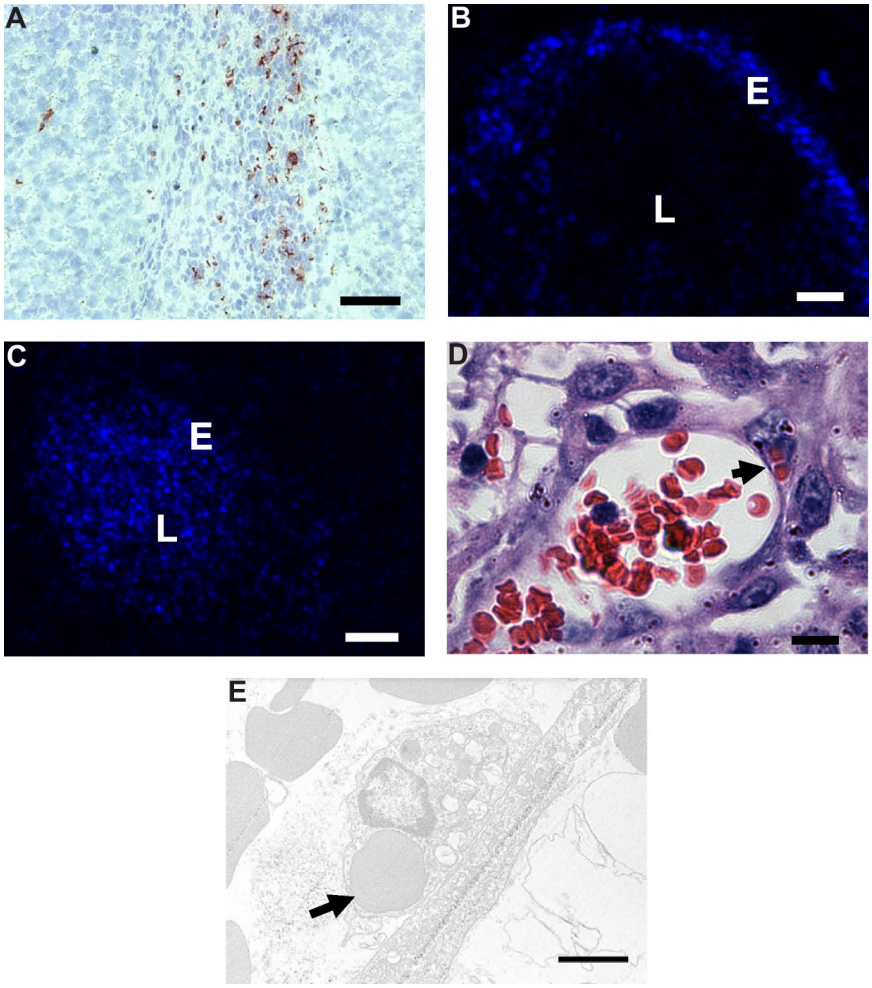

Figure 5. In vivo binding to tumor endothelium and erythrophagocytosis of intravenously administered RGD-erythrocytes in B16.F10 melanoma–bearing mice. (A) Immunohistologic detection of RGD-peptides in tumor tissue, 1 hour after intravenous administration, showing preferential accumulation in the tumor rim. Scale bar represents 200 μm. (B) Fluorescence microscopy image of a tumor blood vessel showing specific binding of RGD-erythrocytes to the vessel wall, 4 hours after intravenous administration of RGD-coupled DiD-labeled erythrocytes. Scale bar represents 30 μm. (C) Fluorescence microscopy image of a tumor blood vessel showing circulating plain DiD-labeled erythrocytes at 4 hours after intravenous administration. Scale bar represents 50 μm. (D) Light microscopy image of a tumor blood vessel showing internalization of multiple erythrocytes by endothelial cells (indicated by arrow) 2 hours after injection. Scale bar represents 10 μm. (E) Transmission electron microscopy image of an erythrocyte phagocytosed by a tumor endothelial cell (indicated by arrow) 4 hours after administration. Scale bar represents 2 μm.

of immunohistochemically stained tumor sections showed anti-RGD staining of RGD-erythrocytes in the tumor periphery (Figure 5A). In liver and spleen, the anti-RGD staining pattern pointed to association with macrophages (Figure S2A,B), which was expected because of integrin-mediated professional phagocyte recognition. In addition, occasional RGD staining of erythrocytes was seen in the lung capillaries (and vessels) but no signs of lung endothelial cell association or any damage were observed (Figure S2C). Examination of fluorescence in tumor tissue following intravenous injection of DiD-labeled RGD-coupled erythrocytes showed preferential binding to the blood vessel wall (Figure 5B). Administration of unmodified erythrocytes presented unspecific lumen staining (Figure 5C).

To study whether RGD-erythrocytes were also phagocytosed by angiogenic endothelial cells in vivo, we sectioned tumors that were excised 2 hours after intravenous injection of RGD-erythrocytes. Light and transmission electron microscopic evaluation revealed phagocytosed RGD-erythrocytes inside the endothelial cells in the blood vessels (Figure 5D,E).

Since RGD-modified erythrocytes show specific binding and internalization by tumor endothelial cells in vivo, we considered that this could evoke serious damage to the endothelial cells. Similarly as observed in vitro, where we noted RGD-erythrocyte–induced cytotoxicity to endothelial cells, physical damage could occur as a result from the uptake of large numbers of erythrocytes inducing (sterical) hindrance of cellular processes. In addition, chemical damage could occur as intraphago(lyso)somal degradation of erythrocytes possibly leads to intracellular release of large amounts of iron, causing intoxication of the endothelial phagocytes.[27]

To explore the possibilities of the occurrence of damaging effects of intravenously injected RGD-erythrocytes on tumor endothelial cells in B16.F10 melanoma–bearing mice, we killed tumor-bearing mice at several time points after RGD-erythrocyte administration. Histologic examination of tumors excised at 4 and 24 hours after administration showed thrombi formation 4 hours after administration (Figure 6A,B) and widespread necrosis in the tumors with a typical viable rim at 24 hours after administration (Figure 6C,D). Appearance of central core necrosis and a remaining viable rim is typically observed for anticancer agents acting through a vascular targeting mechanism of action.[28-30] The observation of the same pattern here supports the theory that RGD-erythrocyte administration induces tumor endothelial cell damage, leading to local thrombi formation and blood vessel occlusion with tumor cell starvation and extensive necrosis as a consequence.

The implication that RGD-erythrocytes are able to induce vascular-damaging effects motivated to us study the antitumor activity in more detail. Tumor-bearing mice received 3 injections of RGD-erythrocytes, every second day. When analyzing tumor size increase during the experiment, tumor growth was delayed for RGD-erythrocytes ($P = .006$) compared with mice treated with RAD-modified erythrocytes (Figure 6E,F).

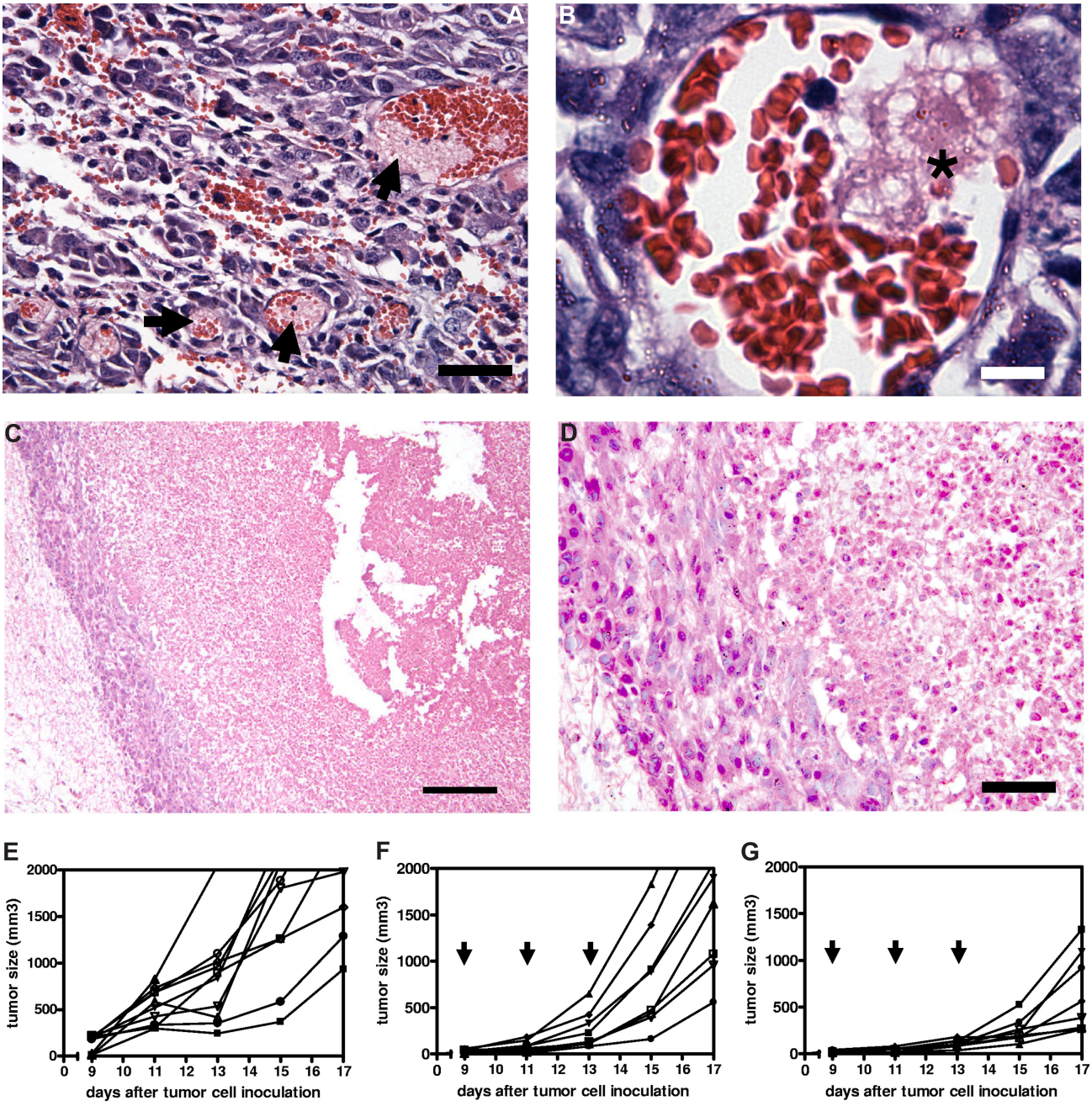

Figure 6. Therapeutic efficacy of tumor endothelium-targeted RGD-erythrocytes in a B16.F10 murine melanoma model. (A) Light microscopy image of tumor tissue showing thrombi formation in blood vessels (indicated by arrows), 4 hours after intravenous injection of RGD-modified erythrocytes. Tumors measured approximately 300 mm^3. Scale bar represents 100 μm. (B) Light microscopy image of a tumor blood vessel showing local thrombus formation (indicated by asterisk) likely due to endothelial cell damage at 2 hours after intravenous injection. Scale bar represents 10 μm. (C) Light microscopy image showing a necrotic tumor core with a typical viable rim at 24 hours after intravenous injection of RGD-modified erythrocytes. Scale bar represents 200 μm. (D) Magnification of viable rim and necrotic tumor area showing a thin layer of cells forming the viable rim. Scale bar represents 50 μm. (E) Individual growth curves (n = 10) of untreated control mice. Mean tumor volume increase during the experiment: 1848 plus or minus 575 mm^3 (mean ± SEM). (F) Individual growth curves (n = 8) after treatment with RAD-modified erythrocytes, arrows indicating day of treatment. Mean tumor volume increase during the experiment: 1787 plus or minus 312 mm^3 (mean ± SEM). (G) Individual growth curves (n = 8) after treatment with RGD-modified erythrocytes, arrows indicating day of treatment. Mean tumor volume increase during the experiment: 636 plus or minus 149 mm^3 (mean ± SEM); $P = .005$ compared with RAD-modified erythrocytes treated animals (Mann-Whitney test, 2 tailed).

Discussion

We have established the binding and phagocytic capacity of angiogenic endothelial cells toward PS-exposing lactadherin-opsonized particles and cells in vitro. These results were confirmed in vivo using artificial RGD-erythrocytes as a model for lactadherin-opsonized particles. We show that the glycoprotein lactadherin is produced in and around tumor blood vessels, which is in line with clinical studies showing increased levels of lactadherin in breast cancer patients, average levels increased from less than 30 to 110 to 280 ng/mL plasma.[31] The expression of lactadherin and α_v-integrins during angiogenesis would place the essential molecules at the scene for angiogenic endothelium-mediated phagocytosis of apoptotic cells. Using a model for apoptotic opsonized cells (by covalently coupling a cyclic RGD-peptide to the erythrocyte outer

surface), we have shown that binding to and phagocytosis of RGD-erythrocytes by angiogenic endothelial cells is indeed occurring both in vitro and in vivo. Inhibition of phagocytosis of RGD-erythrocytes and lactadherin-erythrocytes was confirmed by preincubation of HUVECs with cytochalasin D. Moreover, in vitro binding of lactadherin-erythrocytes could be inhibited by direct competition with RGD-erythrocytes. RGD-erythrocyte binding affinity appeared to be higher, presumably because they have more ligands coupled to their surface compared with the lactadherin erythrocytes as RGD-peptide has a molecular weight of approximately 1 kD, whereas lactadherin is approximately 50 times larger (Mw: 47 kD).

Previous studies demonstrate the possibility of targeting immunoeryth-rocytes in the vascular system: to denuded blood vessel walls and fibrin clots.[32,33] Furthermore, Oka et al showed phagocytosis of aged/apoptotic cells in vitro via a lectinlike oxidized low-density lipoprotein receptor 1 (LOX-1) by bovine aortic endothelial cells (BAEs).[34] Here we show for the first time that erythrocytes are internalized in vivo by a cell type outside the mononuclear phagocyte system (MPS). The RGD-peptide engineered erythrocyte appears to have some additional attractive features for medical applications exploiting the phagocytic potential of angiogenic endothelial cells. We observed that intravenous injection of RGD-erythrocytes resulted in accumulation in the tumor vasculature, suggesting that RGD-erythrocytes may find utility in diagnostic or therapeutic settings. We have shown antitumor effects of RGD-modified erythrocytes in a murine melanoma model, which are likely the consequence of vascular damage. Moreover, antitumor agents can be additionally encapsulated into erythrocytes[21,35] to strengthen their therapeutic impact. Our research also has implications for hematologic disorders such as sickle cell anemia[36] and malaria[37] where the RGD-mediated recognition of PS-exposing erythrocytes contributes to the pathophysiology. In such diseases, the phagocytosis of the erythrocytes has always been attributed to macrophages, but the present study suggests that many of the vascular effects involved in these diseases could be due to interaction of the pathological erythrocytes with the endothelium.

Acknowledgment

The authors thank Prof Dr K. Mertens for critically reading the paper.

Authorship

Contribution: M.H.A.M.F. designed studies, performed the majority of experiments, interpreted experiments, and wrote the paper; E.M. designed in vitro studies and interpreted in vitro experiments; A.M.G. designed microscopy experiments and interpreted microscopy data; F.M.F. and A.U. performed microscopy experiments; J.T.R. provided lactadherin and interpreted data on lactadherin; G.M. interpreted data regarding angiogenic endothelial cells; G.S. supervised the project and wrote the paper; R.M.S. designed experiments, supervised the studies, interpreted data, and wrote the paper.

Conflict-of-interest disclosure: The authors declare no competing financial interests.

Correspondence: R. M. Schiffelers, Room Z735A, Department of Pharmaceutics, Utrecht Institute for Pharmaceutical Sciences (UIPS), Utrecht University, PO Box 80082, 3508 TB Utrecht, The Netherlands; e-mail: r.m.schiffelers@uu.nl.

References

1. Grimsley C, Ravichandran KS. Cues for apoptotic cell engulfment: eat-me, don't eat-me and come-get-me signals. Trends Cell Biol. 2003;13:648-656.
2. Wu Y, Tibrewal N, Birge RB. Phosphatidylserine recognition by phagocytes: a view to a kill. Trends Cell Biol. 2006;16:189-197.
3. Hoffmann PR, deCathelineau AM, Ogden CA, et al. Phosphatidylserine (PS) induces PS receptor-mediated macropinocytosis and promotes clearance of apoptotic cells. J Cell Biol. 2001;155:649-659.
4. Stubbs JD, Lekutis C, Singer KL, et al. cDNA cloning of a mouse mammary epithelial cell surface protein reveals the existence of epidermal growth factor-like domains linked to factor VIII-like sequences. Proc Natl Acad Sci U S A. 1990; 87:8417-8421.
5. Hanayama R, Tanaka M, Miwa K, Shinohara A, Iwamatsu A, Nagata S. Identification of a factor that links apoptotic cells to phagocytes. Nature. 2002;417:182-187.
6. Akakura S, Singh S, Spataro M, et al. The opsonin MFG-E8 is a ligand for the alphavbeta5 integrin and triggers DOCK180-dependent Rac1 activation for the phagocytosis of apoptotic cells. Exp Cell Res. 2004;292:403-416.
7. Andersen MH, Graversen H, Fedosov SN, Petersen TE, Rasmussen JT. Functional analyses of two cellular binding domains of bovine lactadherin. Biochemistry. 2000;39:6200-6206.
8. Ren Y, Savill J. Apoptosis: the importance of being eaten. Cell Death Differ. 1998;5:563-568.
9. Asano K, Miwa M, Miwa K, et al. Masking of phosphatidylserine inhibits apoptotic cell engulfment and induces autoantibody production in mice. J Exp Med. 2004;200:459-467.
10. Hanayama R, Tanaka M, Miyasaka K, et al. Autoimmune disease and impaired uptake of apoptotic cells in MFG-E8-deficient mice. Science. 2004; 304:1147-1150.
11. Savill J, Dransfield I, Hogg N, Haslett C. Vitronectin receptor-mediated phagocytosis of cells undergoing apoptosis. Nature. 1990;343:170-173.
12. Hu P, Yan J, Sharifi J, Bai T, Khawli LA, Epstein AL. Comparison of three different targeted tissue factor fusion proteins for inducing tumor vessel thrombosis. Cancer Res. 2003;63:5046-5053.
13. Hynes RO. Integrins: versatility, modulation, and signaling in cell adhesion. Cell. 1992;69:11-25.
14. Eliceiri BP, Cheresh DA. The role of alphav integrins during angiogenesis: insights into potential mechanisms of action and clinical development. J Clin Invest. 1999;103:1227-1230.
15. Silvestre JS, Thery C, Hamard G, et al. Lactadherin promotes VEGF-dependent neovascularization. Nat Med. 2005;11:499-506.
16. Hvarregaard J, Andersen MH, Berglund L, Rasmussen JT, Petersen TE. Characterization of glycoprotein PAS-6/7 from membranes of bovine milk fat globules. Eur J Biochem. 1996;240:628-636.
17. Coller BS, Springer KT, Beer JH, et al. Thromboerythrocytes: in vitro studies of a potential autologous, semi-artificial alternative to platelet transfusions. J Clin Invest. 1992;89:546-555.
18. Kok RJ, Schraa AJ, Bos EJ, et al. Preparation and functional evaluation of RGD-modified proteins as alpha(v)beta(3) integrin directed therapeutics. Bioconjug Chem. 2002;13:128-135.
19. Temming K, Meyer DL, Zabinski R, et al. Evaluation of RGD-targeted albumin carriers for specific delivery of auristatin E to tumor blood vessels. Bioconjug Chem. 2006;17:1385-1394.
20. Neutzner M, Lopez T, Feng X, Bergmann-Leitner ES, Leitner WW, Udey MC. MFG-E8/lactadherin promotes tumor growth in an angiogenesis-dependent transgenic mouse model of multistage carcinogenesis. Cancer Res. 2007;67:6777-6785.
21. Rossi L, Serafini S, Pierige F, et al. Erythrocyte-based drug delivery. Expert Opin Drug Deliv. 2005;2:311-322.
22. Desai AG, Thakur ML. Radiolabeled blood cells: techniques and applications. Crit Rev Clin Lab Sci. 1986;24:95-122.
23. Boas FE, Forman L, Beutler E. Phosphatidylserine exposure and red cell viability in red cell aging and in hemolytic anemia. Proc Natl Acad Sci U S A. 1998;95:3077-3081.
24. Aderem A Phagocytosis and the inflammatory response. J Infect Dis. 2003;187(suppl 2):S340-S345.
25. Araki N, Johnson MT, Swanson JA. A role for phosphoinositide 3-kinase in the completion of macropinocytosis and phagocytosis by macrophages. J Cell Biol. 1996;135:1249-1260.
26. Schrijvers DM, Martinet W, De Meyer GR, Andries L, Herman AG, Kockx MM. Flow cytometric evaluation of a model for phagocytosis of cells

undergoing apoptosis. J Immunol Methods. 2004; 287:101-108.

27. Balla J, Vercellotti GM, Nath K, et al. Haem, haem oxygenase and ferritin in vascular endothelial cell injury. Nephrol Dial Transplant. 2003; 18(suppl 5):v8-v12.
28. Thorpe PE. Vascular targeting agents as cancer therapeutics. Clin Cancer Res. 2004;10:415-427.
29. Davis PD, Dougherty GJ, Blakey DC, et al. ZD6126: a novel vascular-targeting agent that causes selective destruction of tumor vasculature. Cancer Res. 2002;62:7247-7253.
30. Tozer GM, Kanthou C, Baguley BC. Disrupting tumour blood vessels. Nat Rev Cancer. 2005;5: 423-435.
31. Ceriani RL, Sasaki M, Sussman H, Wara WM, Blank EW. Circulating human mammary epithelial antigens in breast cancer. Proc Natl Acad Sci U S A. 1982;79:5420-5424.
32. Muzykantov VR, Sakharov DV, Smirnov MD, Samokhin GP, Smirnov VN. Immunotargeting of erythrocyte-bound streptokinase provides local lysis of a fibrin clot. Biochim Biophys Acta. 1986; 884:355-362.
33. Smirnov VN, Domogatsky SP, Dolgov VV, et al. Carrier-directed targeting of liposomes and erythrocytes to denuded areas of vessel wall. Proc Natl Acad Sci U S A. 1986;83:6603-6607.
34. Oka K, Sawamura T, Kikuta K, et al. Lectin-like oxidized low-density lipoprotein receptor 1 mediates phagocytosis of aged/apoptotic cells in endothelial cells. Proc Natl Acad Sci U S A. 1998; 95:9535-9540.
35. Magnani M, Rossi L, D'Ascenzo M, Panzani I, Bigi L, Zanella A. Erythrocyte engineering for drug delivery and targeting. Biotechnol Appl Biochem. 1998;28(pt 1):1-6.
36. Kumar A, Eckman JR, Wick TM. Inhibition of plasma-mediated adherence of sickle erythrocytes to microvascular endothelium by conformationally constrained RGD-containing peptides. Am J Hematol. 1996;53:92-98.
37. Eda S, Lawler J, Sherman IW. Plasmodium falciparum-infected erythrocyte adhesion to the type 3 repeat domain of thrombospondin-1 is mediated by a modified band 3 protein. Mol Biochem Parasitol. 1999;100:195-205.